Vascular niche promotes hematopoietic multipotent progenitor formation from pluripotent stem cells

Jennifer L. Gori,[1] Jason M. Butler,[2,3] Yan-Yi Chan,[1] Devikha Chandrasekaran,[1] Michael G. Poulos,[2,3] Michael Ginsberg,[4] Daniel J. Nolan,[4] Olivier Elemento,[5] Brent L. Wood,[6,7] Jennifer E. Adair,[1,8] Shahin Rafii,[9] and Hans-Peter Kiem[1,6,8]

[1]Clinical Research Division, Fred Hutchinson Cancer Research Center (FHCRC), Seattle, Washington, USA. [2]Department of Genetic Medicine, Ansary Stem Cell Institute, and [3]Department of Surgery, Weill Cornell Medical College, New York, New York, USA. [4]Angiocrine Bioscience, New York, New York, USA. [5]HRH Prince Alwaleed Bin Talal Bin Abdulaziz Alsaud Institute for Computational Biomedicine, Weill Cornell Medical College, New York, New York, USA. [6]Department of Pathology, [7]Department of Laboratory Medicine, and [8]Department of Medicine, University of Washington, Seattle, Washington, USA. [9]Howard Hughes Medical Institute, Ansary Stem Cell Institute, Department of Genetic Medicine, Weill Cornell Medical College, New York, New York, USA.

Pluripotent stem cells (PSCs) represent an alternative hematopoietic stem cell (HSC) source for treating hematopoietic disease. The limited engraftment of human PSC–derived (hPSC-derived) multipotent progenitor cells (MPP) has hampered the clinical application of these cells and suggests that MPP require additional cues for definitive hematopoiesis. We hypothesized that the presence of a vascular niche that produces Notch ligands jagged-1 (JAG1) and delta-like ligand-4 (DLL4) drives definitive hematopoiesis. We differentiated hes2 human embryonic stem cells (hESC) and *Macaca nemestrina*–induced PSC (iPSC) line-7 with cytokines in the presence or absence of endothelial cells (ECs) that express JAG1 and DLL4. Cells cocultured with ECs generated substantially more $CD34^+CD45^+$ hematopoietic progenitors compared with cells cocultured without ECs or with ECs lacking JAG1 or DLL4. EC-induced cells exhibited Notch activation and expressed HSC-specific Notch targets *RUNX1* and *GATA2*. EC-induced PSC-MPP engrafted at a markedly higher level in NOD/SCID/IL-2 receptor γ chain–null (NSG) mice compared with cytokine-induced cells, and low-dose chemotherapy-based selection further increased engraftment. Long-term engraftment and the myeloid-to-lymphoid ratio achieved with vascular niche induction were similar to levels achieved for cord blood–derived MPP and up to 20-fold higher than those achieved with hPSC-derived MPP engraftment. Our findings indicate that endothelial Notch ligands promote PSC-definitive hematopoiesis and production of long-term engrafting $CD34^+$ cells, suggesting these ligands are critical for HSC emergence.

Introduction

Hematopoietic disease affects millions of people worldwide. In many cases, transplantation of healthy or genetically corrected long-term engrafting hematopoietic stem cells (LT-HSCs) is the only cure. Finding a suitable allogeneic HLA-matched donor is a formidable challenge, and there are considerable side effects associated with allogeneic transplantation. Gene therapy of autologous LT-HSCs is another emerging option; however, difficulty collecting sufficient numbers of cells from the BM, the lack of an efficient ex vivo expansion condition that maintains LT-HSCs, and patient health have impeded autologous stem cell gene therapy. While pluripotent stem cells (PSCs), which include autologous induced PSCs (iPSCs) and allogeneic embryonic stem cells (ESCs), are a theoretically unlimited source of HSCs, use of this technology for blood stem cell therapy is hampered by the restricted engraftment and reconstitution potential of human PSC–derived (hPSC-derived) multipotent progenitor cells (MPP) observed in mouse xenografts over the past 10 years (1–5). This substantial barrier has delayed clinical translation of PSC-based blood therapeutics. As a result, the focus of pluripotent blood stem cell therapy research has shifted to identifying developmental mechanisms and molecular pathways that drive hematopoietic specification from hemogenic endothelial precursors, with an emphasis on zebrafish and mouse models (6–10).

In the last few years, evidence describing a key role for endothelial cells (ECs) in HSC development, homeostasis, and regeneration has been accumulating (11–13). ECs form putative "vascular niches" that influence HSC development and maintenance, from the first definitive HSCs that emerge from the ventral wall of the dorsal aorta (6) to the ECs in the BM microenvironment that produce prohematopoietic Notch ligand jagged-1 (JAG1), which is required for homeostatic and regenerative hematopoiesis (14). Rafii et al. showed that transduction of vascular endothelium with the *E4ORF1* gene, which activates the Akt pathway in human ECs, augments human long-term MPP (LT-MPP) expansion through paracrine cues along key signaling pathways, including the Notch pathway (12, 15, 16). We therefore hypothesized that Notch ligands deployed by ECs are involved in definitive hematopoietic specification and thus an ex vivo vascular niche would support formation of definitive LT-MPP from PSC hemogenic precursors. We focused primarily on the nonhuman primate (NHP) *Macaca nemestrina* (Mn) iPSC model (17–19), which provides the means for evaluating MPP fate in xenograft mouse studies and also allows for the future testing in a clinically relevant autologous setting in the NHP. To

Conflict of interest: Shahin Rafii is the founder of Angiocrine Bioscience. He is on the scientific advisory board and holds equity in the company. Daniel J. Nolan and Michael Ginsberg are employees and equity holders in Angiocrine Bioscience.
Submitted: October 13, 2014; **Accepted:** January 5, 2015.
Reference information: *J Clin Invest*. doi:10.1172/JCI79328.

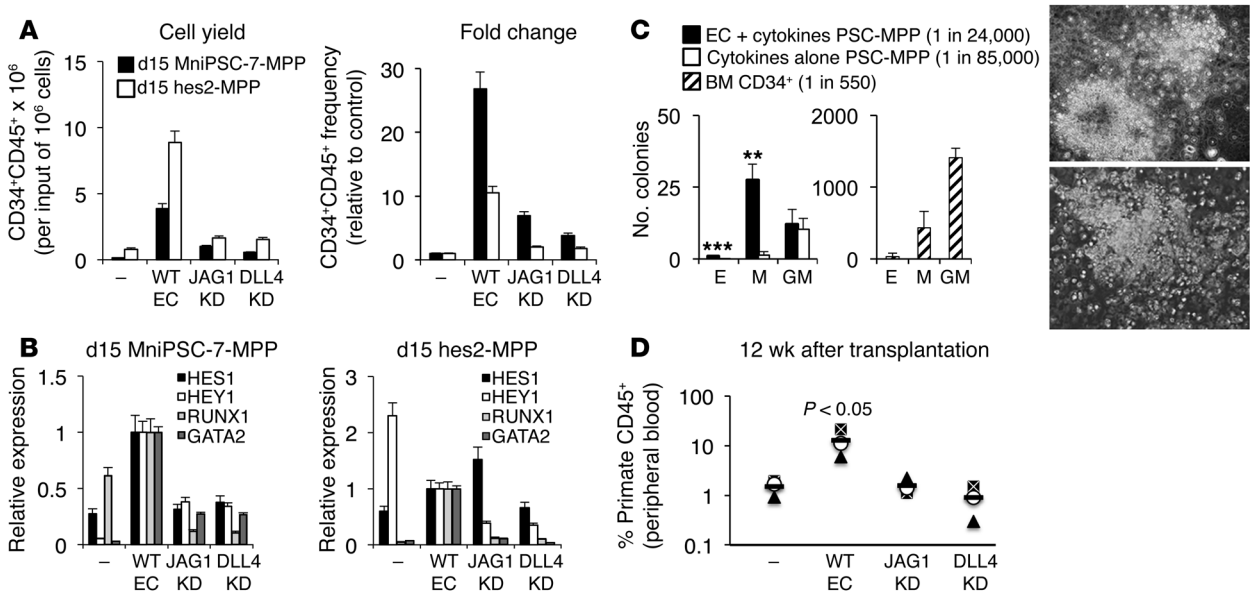

Figure 1. Endothelial Notch ligands regulate emergence and expansion of hematopoietic progenitor cells from PSCs. (**A**) Left: CD34⁺CD45⁺ cell yield per million input of cells ± ECs and Notch ligand– replete and –depleted conditions. Right: fold change in CD34⁺CD45⁺ cells relative to MPP generated in cytokines. JAG1-KD, ECs transduced with shRNA to JAG1; DLL4-KD, ECs transduced with shRNA to DLL4, –, cytokines alone. (**B**) Notch signaling target expression on day 15. Left: MniPSC-7–MPP; right: day hes2-MPP after coculture in indicated conditions. Levels calibrated to expression in PSC-MPP cocultured with WT ECs and normalized to β-actin. (**C**) Number of hematopoietic CFUs from day-15 MniPSC-7–MPP after expansion ± WT ECs. Right: Mn BM CD34⁺ activity (control). CFUs per 100,000 cells plated. Plating efficiency noted in parentheses. Far right: CFUs from day 15 MniPSC-7–MPP and BM CD34⁺ cells. Original magnification, ×20. (**D**) Primate CD45⁺ cells in blood 12 weeks after transplantation (1 transplant experiment, $n = 3$ mice/group, bars represent mean/group). $^{**}P < 0.005$; $^{***}P < 0.0005$, Student's t test. Differentiation studies ± Notch ligand–depleted ECs were conducted in 2 MniPSC lines and 1 hESC line (hes2) in 3 independent experiments per cell line. Differentiation studies comparing induction with cytokines alone and WT ECs were conducted in 2 MniPSC lines and 1 hESC line in 6 independent experiments per cell line.

determine the mechanism of action of vascular niche induction of hematopoiesis and to allow for translation to human cell studies for future development toward clinical application, we also tested differentiation and engraftment with human ESCs (hESCs) with and without EC-mediated Notch pathway activation. Here, we identify a role for endothelial Notch ligands JAG1 and delta-like ligand-4 (DLL4) in the emergence of LT-MPP in definitive hematopoiesis.

Results

EC notch ligands JAG1 and DLL4 activate Notch signaling, RUNX1, and GATA2 expression in PSC hematopoietic progenitors and emergence of CD34⁺CD45⁺ cells with ex vivo and in vivo hematopoietic activity. To direct hemogenic mesoderm induction of human and NHP PSCs, we used an 8-day staged protocol based on our previously established strategy (ref. 17 and Supplemental Figure 1A; supplemental material available online with this article; doi:10.1172/JCI79328DS1). The cell lines used in these experiments are the hESC line hes2 from the WiCell Research Institute, which has been previously characterized (20) and has been used to study hematopoiesis ex vivo (21), and the NHP lines MniPSC-7 and MniPSC-3, which were generated in our laboratory and have been previously characterized (17, 19). hes2 and MniPSC-7 were aggregated in media containing 10 ng/ml and 20 ng/ml human BMP4, respectively. Embryoid body (EB) aggregates were then exposed to VEGF, bFGF, and PGE2, the latter of which we previously showed to enhance emergence of CD34⁺CD45⁺ cells when added during the first week of hematopoietic differentiation (17). By day 8 of induction, 35% of hes2 and 20% of MniPSC-7 hematopoietic progenitors expressed the hematoendothelial marker CD34 and 80% of the CD34⁺ fraction also expressed the endothelial surface antigens Flk1 (KDR), CD31 (PECAM-1), and VE-cadherin (Supplemental Figure 1B). CD45⁻PECAM1⁺Flk-1⁺VE-cadherin (CD45^{neg}PFV) cells have been shown to represent a bipotent population generated from hESC that is responsible for hematopoietic fate (22). Previous work from several groups shows that hematoendothelial precursors specified toward hematopoietic fate by coculture with growth factors alone (23–25) or with stromal cell support (2, 26) give rise to phenotypic but primitive hematopoietic progenitors that lack robust, long-term multilineage engraftment potential.

We hypothesized that ECs, which are the initial site of definitive hematopoiesis and express the membrane-bound Notch ligands JAG1 and DLL4, control the transition from PSC-derived hemogenic precursor to definitive HSC. Given that JAG1 and DLL4 compete for binding of Notch-1 and Notch-2 receptors and have opposing effects on ECs during angiogenesis (27), we further postulated that a balance of endothelial JAG1 and DLL4 ligands is required for HSC emergence.

To test our hypothesis, we transduced ECs with lentivirus vectors expressing shRNAs to JAG1 and DLL4 (knockdown [KD]) for use in our coculture differentiation strategy. KD of JAG1 and DLL4 was confirmed by quantitative reverse-transcriptase PCR (qRT-PCR) and by flow cytometry analysis (Supplemental Figure 1C and data not shown). Day-8 PSC-derived CD34⁺ cells expressed Notch-1 and Notch-2 receptors and other receptors (*TIE1*, *TIE2*,

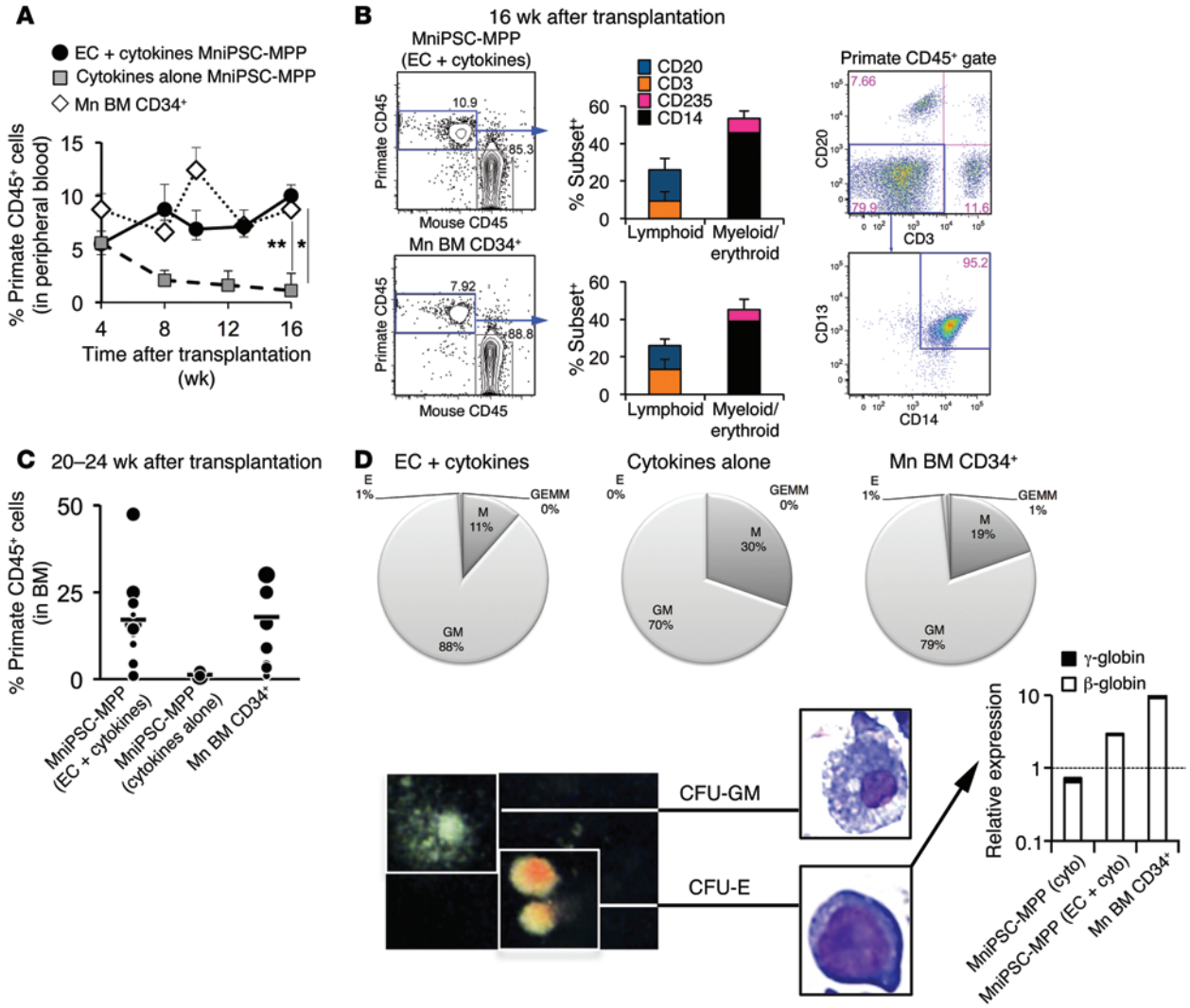

Figure 2. Long-term multilineage engraftment of vascular niche–induced MniPSC-MPP. Detection of primate CD45+ cells in blood of mice transplanted with EC-induced MniPSC-MPP, cytokine-induced MniPSC-MPP, or Mn BM CD34+ cells. (**A**) Kinetics of primate CD45+ cells in blood. *$P < 0.05$; **$P < 0.005$, Student's *t* test. (**B**) Distinction between primate and mouse CD45+ cells by flow cytometry analysis. Middle panels: lymphoid and myeloid subset analysis. Right panels: flow cytometry plots showing CD3, CD20 single-positive and CD13, CD14 double-positive cells. (**C**) Primate CD45+ cells in BM. Dots indicate individual mice. Lines show mean/group. (**D**) Top panels: frequency of BM CFUs. M, macrophage; GM, granulocyte-macrophage; E, erythroid; GEMM,mixed. Bottom panels: colonies from BM of EC MniPSC-MPP mouse. Original magnification, ×4. Middle panels: Wright-stained macrophage and erythroid cells. Original magnification, ×20. Right panels: qRT-PCR for primate γ- and β-hemoglobin from erythroid (BFU-E) cells. Transcripts normalized to β-actin and calibrated to macaque blood (line indicates calibrator level). Transplantation studies were conducted in 8 to 12 mice/group over 3 independent experiments.

IGFR) that are required to transduce signals upon interaction with endothelium (Supplemental Figure 1D). Day-8 CD34+ cells were replated in StemSpan media supplemented with prohematopoietic cytokines with or without vascular niche support to induce hematopoietic specification. KD of either JAG1 or DLL4 in the ECs significantly reduced the CD34+CD45+ cell yield (Figure 1A and Supplemental Figure 1B). PSC-MPP cultured with WT ECs had 8-fold higher CD34+CD45+ cell yield (per input of 1 million cells) compared with cells specified with cytokines alone. EC coculture had a greater impact on the frequency of CD34+CD45+ cells produced from MniPSC compared with hes2 hemogenic precursors, with a 30-fold and a 10-fold increase, respectively, compared with cells induced with cytokines alone. KD of either JAG1 or DLL4 significantly reduced the CD34+CD45+ cell yield (Figure 1A). Importantly, cells cultured with JAG1-KD and DLL4-KD ECs also exhibited reduced Notch activation, as indicated by lower expression of Notch targets *HES1*, *HEY1*, *RUNX1,* and *GATA2* (Figure 1B), the latter 2 of which are required for definitive hematopoiesis (*RUNX1*: refs. 9, 28; *GATA2*: refs. 29, 30). To show that the effect of vascular niche coculture was not an artifact of the line MniPSC-7, experiments were repeated with another MniPSC line (MniPSC-3) with similar results (Supplemental Figure 1, D and E).

RNA-Seq analysis also confirmed increased expression of Notch-1 and Notch-2 downstream targets (*HES1*, *HEY1*, *ADAM10*, *GATA2*) for vascular niche–induced, but not cytokine–induced, MniPSC-MPP (Supplemental Figure 2). Comparative transcriptome analysis (by hierarchical clustering and 3D scaling analysis) identified several greater than 4-fold differentially expressed

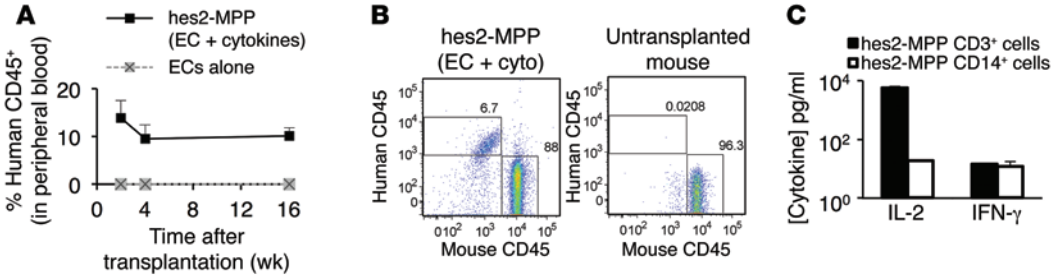

Figure 3. hESCs differentiated in a vascular niche give rise to engrafting MPP with in vivo myeloid and lymphoid potential. (**A**) Kinetics of EC-induced hes2-MPP engraftment compared with mice transplanted with ECs alone. (**B**) Distinction between the human and mouse CD45. (**C**) Th1 cytokine production by human CD3+ cells and CD14+ cells. For cytokine assays, cells were isolated from organs of 3 mice/group (3 biological replicates) and 3 technical replicates were run for each test.

genes in EC-induced, but not cytokine-induced, cells, including regulators of HSC transcription, adhesion/migration, vascular genes, and hematopoiesis (Notch, TGF-β, Wnt), indicating that hematopoietic specification in a vascular niche is also associated with a distinct transcriptional profile.

Vascular niche–induced MniPSC-MPP also had significantly more hematopoietic activity, both ex vivo and in vivo. Colony-forming assays indicated that vascular niche–induced hematopoietic cells gave rise to significantly more erythroid (CFU-E) and myeloid (CFU-M) colonies and had a higher plating efficiency compared with cells induced with cytokines alone (Figure 1C). However, both PSC-derived hematopoietic cell populations had lower colony-forming potential compared with somatic CD34+ cells isolated from monkey BM (positive control). To determine the effect of endothelial Notch ligand induction on emergence of engraftable hematopoietic cells, cocultures of day-15 MniPSC-7 hematopoietic progenitors with or without Notch ligand–depleted (JAG1-KD or DLL4-KD) or WT ECs (n = 3 mice per group) were injected directly into the BM of immunodeficient NOD/SCID/IL-2 receptor γ chain–null (NSG) mice. Mice transplanted with MniPSC hematopoietic cells that were induced/coinfused with WT ECs had significantly higher engraftment of primate CD45+ cells 12 weeks after transplantation, compared with recipients of cytokine-induced cells and recipients of cells induced with cytokines and JAG1-KD or DLL4-KD ECs (Figure 1D). Together, these data show that generation of hematopoietic progenitors is more robust in the context of a vascular niche and that KD of either pro-HSC Notch ligand JAG1 or proangiogenic Notch ligand DLL4 impedes hematopoietic specification and emergence of engraftable MPP, indicating a direct role for endothelial membrane–bound Notch ligands JAG1 and DLL4 in HSC emergence.

Long-term engraftment of vascular niche iPSC–derived MPP. Several research groups have generated hPSC-derived hematopoietic cells that resemble MPP (2, 4, 5), but that do not engraft long-term and/or lack lymphoid potential in vivo. We hypothesized that vascular niche induction of hematopoiesis would facilitate hemogenic precursor maturation to LT-MPP. To evaluate long-term (>20 week) engraftment potential of PSC-derived cells, MniPSC-MPP/EC cocultures, Mn BM CD34+ cells (positive control for MniPSC-MPP), or cytokine-expanded MniPSC-MPP were injected into the BM of NSG mice (Supplemental Figure 3A). Cells were pulsed with PGE2 prior to intra-BM injection in order to promote homing to and lodgment in the BM. Treatment of HSCs with PGE2 increases CXCR4 expression and has been shown to improve BM engraftment in the clinic (31, 32). Pulsing PSC-MPP with PGE2 increased expression of CXCR4 on MniPSC and hes2 day-15 hematopoietic progenitors (Supplemental Figure 4).

Two weeks after transplantation, NHP CD45+ cells were detected in the blood of all mice transplanted with PSC-derived hematopoietic cells. By week 16, engraftment stabilized at approximately 10% primate CD45+ cells detected in the blood of the recipients of Mn BM CD34+ cell and endothelial-induced MniPSC-MPP (Figure 2A), which is similar to what has been reported for human umbilical cord blood MPP (UCB-MPP) and what we observed with pigtail macaque UCB-MPP after xenotransplantation in NSG mice (33). In contrast, mice transplanted with cytokine-induced MniPSC-MPP had approximately 1% engraftment by week 16.

In vivo hematopoietic subset analysis revealed that lymphoid (CD3, CD20), myeloid (CD13, CD14), and erythroid subsets were detected in the peripheral blood, with no significant differences between PSC-MPP– and BM-derived somatic CD34+ cell recipients (Figure 2B). Importantly, the myeloid-to-lymphoid ratio (M/L) for MniPSC-MPP and Mn BM-MPP (M/L 2/1.7) was similar to what is observed in UCB-MPP–transplanted mice (M/L 1–2) (16, 34, 35). From 20 to 24 weeks after transplantation, CD45+ cell content in the BM was equivalent between the MniPSC-MPP and BM-MPP recipient mice (~20%) compared with 1% engraftment in mice transplanted with cytokine-induced cells (Figure 2B). BM cells from primary recipients were then plated in primate colony-forming cell (CFC) assays to assess myeloid and erythroid potential of long-term engrafted cells (Figure 2C). EC-induced engrafted cells gave rise to both erythroid and myeloid colonies that had characteristic colony and cell morphology. While the percentage of colony types (i.e., CFU-GM) were similar between engrafted EC-induced MniPSC-MPP and somatic CD34+ cells, engrafted cytokine-induced cells had more CFU-M colonies and less than 1% CFU-E colonies detected (Figure 2D, percentages < 1% not shown). qRT-PCR analysis of erythroid cells indicated predominant expression of β-globin (and relatively lower expression of γ-globin), suggesting globin switching occurred in vivo. However, a lower level of β-globin was detected in erythroid cells from recipients of cytokine-induced MPP.

To confirm that the progeny of engrafted MniPSC-MPP are functionally indistinct from the progeny of somatic CD34+ cells, we isolated human and NHP CD3+ cells from the spleen and CD14+ cells from the BM of transplanted mice (Supplemental Figure 3, B and C). Splenic CD3+ cells from PSC-MPP– and somatic BM CD34+–transplanted mice proliferated ex vivo in response to CD3/CD28 immunomagnetic bead activation and coexpressed CD3 and TCR-αβ. CD14+ cells isolated from the BM differentiated into macrophages ex vivo and became activated after treatment with

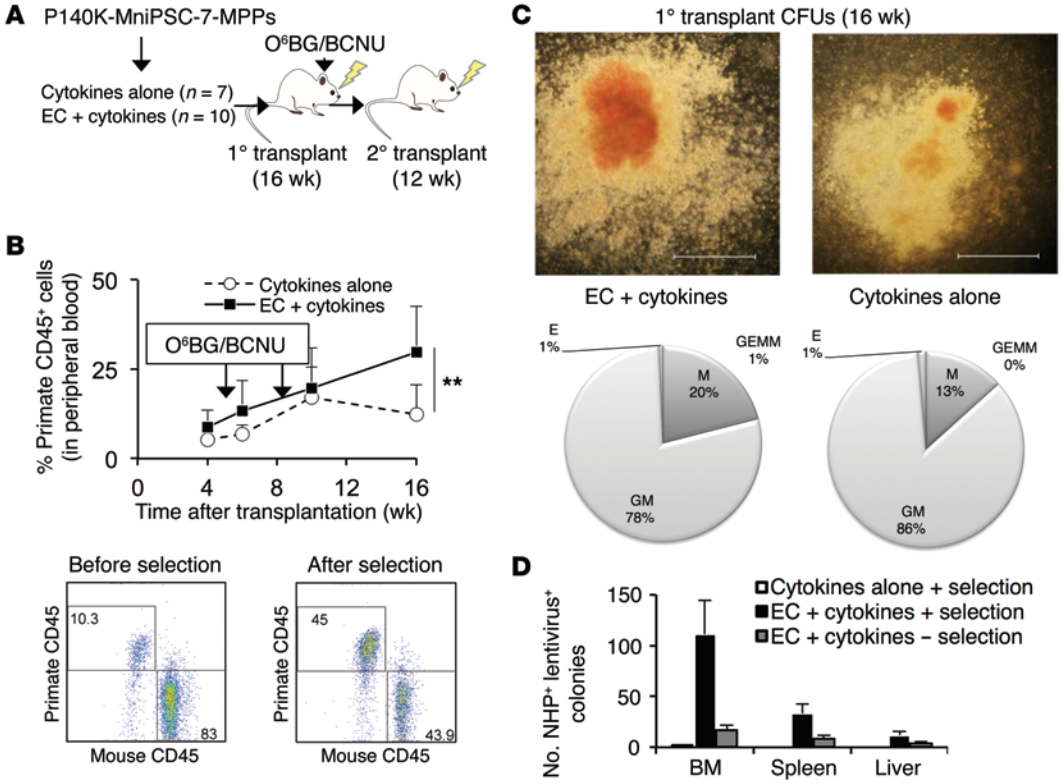

Figure 4. In vivo selection increases long-term engraftment of EC-induced MniPSC-MPP. (**A**) Experimental schematic. (**B**) In vivo selection of EC-expanded MniPSC-MPP (n = 10) versus cytokine-expanded MniPSC-MPP (n = 7). Arrows indicate O^{6}BG/BCNU. Primate CD45$^+$ cells in EC-induced MniPSC-MPP–transplanted mouse before and after in vivo selection (4 and 16 weeks, respectively). (**C**) CFU-GEMM from BM of EC-induced MniPSC-MPP–transplanted mice. Original magnification, ×20. Scale bars: 100 μm. Bottom panels: CFU frequencies in primary recipient BM. (**D**) Summary of gene marking by PCR in organs. Values are mean of biological replicates (mean ± SD for all mice/group). Transplantation studies were conducted in 8 to 12 mice/group over 2 independent experiments. $^{**}P < 0.005$, Student's t test.

lipopolysaccharide. To evaluate cell functionality, we quantified cytokine production after activation; Th1 cytokines (IL-2, IFN-γ) were detected in the activated CD3 and CD14 cells isolated from mice transplanted with EC-induced MPP (Supplemental Figure 3C). In contrast, we could not isolate or activate a sufficient quantity of CD3$^+$ cells to detect Th1 cytokines from the mice engrafted with cytokine-induced MPP.

In order to determine whether this technology is translatable to human cells, hemogenic cells from the hESC line hes2 were also induced with the vascular endothelial platform and then tested for engraftment. A group of mice transplanted with human ECs alone was also included to confirm that the vascular niche cells alone were not the engrafting cell type. Vascular niche–induced hes2-MPP engrafted at a level similar to what was observed with EC-induced MniPSC-MPP (~10%, 16 weeks after infusion) and the isolated hematopoietic progeny were also responsive to activation, producing Th1 cytokines (Figure 3). In contrast, no human CD45$^+$ cells were detected in the mice transplanted with vascular niche cells alone. Together, these data indicate that vascular niche induction of PSC hematopoiesis supports emergence of long-term engrafting definitive multipotent hematopoietic progenitors that give rise to functional hematopoietic progeny in vivo.

EC coinfusion with MniPSC-MPP without prior coculture is not sufficient to promote long-term multilineage hematopoiesis in vivo. To determine whether the direct contact with EC in coculture is required for acquisition multipotency and self-renewal properties, MniPSC-MPP were specified with cytokines alone (grown without EC contact) and then coinfused with ECs. These cells preferentially engrafted in the liver, which is similar to engraftment patterns seen with hPSC–derived primitive hematopoietic cells and indicates that vascular niche induction of definitive hematopoiesis occurs during coculture and is required for acquisition of HSC-like properties (data not shown). This finding is also consistent with our previous work, which showed that cell-to-cell contact between hematopoietic cells and ECs is required for LT-MPP maintenance and expansion (12, 14–16).

In vivo selection of P140K-MGMT gene-modified PSC-MPP by treatment with low-dose O^{6}BG/BCNU chemotherapy increases polyclonal long-term engraftment. Although 10% engraftment of PSC-MPP 16 weeks after transplantation has not been previously achieved, we wanted to improve upon this clinically applicable engraftment threshold. We hypothesized that engineering PSC to express a chemotherapy-resistance transgene would allow for in vivo selection to provide the engrafting cells with a selective advantage for repopulation in order to stabilize and increase long-term engraftment to a desired therapeutic level. To test our hypothesis, we gene modified MniPSC with a chemotherapy-resistance transgene (P140K variant of methylguanine methyltransferase, MGMT), which we have previously shown allows for in vivo selection in NHP and clinical studies (36–38). After validation of

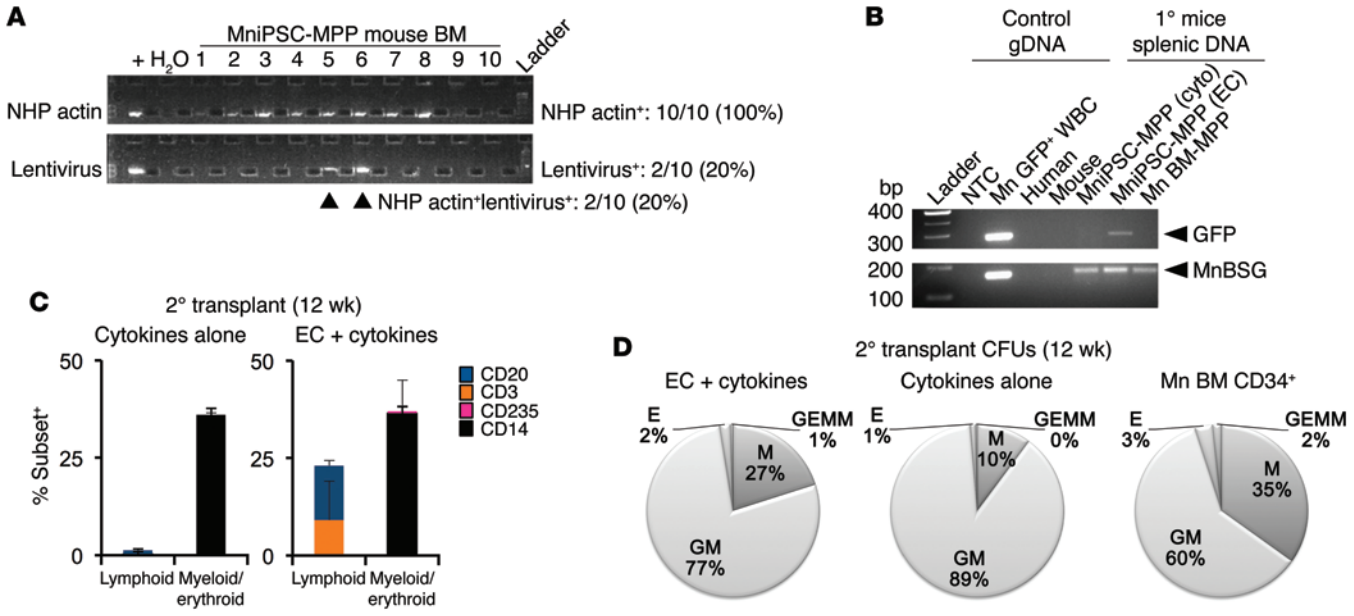

Figure 5. Gene-modified MniPSC-MPP from primary recipient mouse BM reconstitute secondary recipient mice. (**A**) Representative PCR analysis of mouse BM from EC-MniPSC-MPP mouse for data shown in Figure 4D showing detection of primate β-actin and lentivirus LTR. (**B**) PCR of GFP transgene (top gel) and macaque (Mn) BSG (lower gel) in gDNA from GFP+ sorted monkey PBMCs, unmodified, negative control human and mouse hematopoietic cells, and splenic gDNA from representative engrafted mice. (**C**) Subsets in second-degree recipients. (**D**) CFUs from BM of second-degree recipient mice. Secondary transplantation studies were conducted in 3 mice/group over 2 independent experiments.

P140K-MGMT transgene expression at the protein and RNA levels (Supplemental Figure 5, A and B; Supplemental Uncut Gel Image 1), resistance to alkylating chemotherapy was evaluated in P140K+ and P140K- MniPSC-derived hematopoietic cells (Supplemental Figure 5C). Day-8 hemogenic CD34+ cells were plated in CFC assays after treatment with vehicle or O6-benzylguanine (O6BG) with or without N,N′-Bis(2-chloroethyl)-1-nitrosourea (BCNU) chemotherapy. P140K+ MniPSC–derived cells maintained significantly more hematopoietic colony-forming potential compared with P140K- MniPSC–derived cells after chemotherapy exposure (*$P < 0.05$). To determine clonality of the gene-modified cells, we performed retroviral integration site (RIS) analysis that identified 148 unique clones in P140K+ MniPSC over several passages in culture, indicating that the P140K+ MniPSC line is highly polyclonal (Supplemental Figure 5D).

To evaluate in vivo hematopoietic potential and to determine whether O6BG/BCNU chemotherapy would increase engraftment of gene-modified cells, we generated hematopoietic progenitors from P140K+ MniPSC by differentiation with cytokines with or without ECs and then transplanted these cell populations into NSG mice (Figure 4A). Four weeks after transplantation, there was no difference in the short-term engraftment of MniPSC-MPP with or without ECs (Figure 4B). In vivo selection by 2 treatments with low-dose O6BG/BCNU (5 and 9 weeks after transplantation) increased primate CD45+ engraftment levels. In vivo selection in mice transplanted with EC-induced MniPSC-MPP was significantly more effective compared with selection in mice transplanted with cytokine-induced cells, as indicated by the 4-fold increase in engraftment (30% primate CD45+ in peripheral blood) (Figure 4B), which was sustained until the end of the study ($P < 0.005$).

Sixteen weeks after transplantation, engraftment and gene marking were evaluated in hematopoietic organs. Up to 60% of primate CD45+ cells were detected in BM of EC-induced MniPSC-MPP recipients, which is significantly higher compared with cytokine-expanded cells. To confirm gene marking, hematopoietic CFU assays were established from mouse BM, spleen, and liver (Figure 4, C and D). Mixed CFU–granulocyte, erythroid, macrophage, megakaryocyte (CFU-GEMM) colonies grew from BM cells from mice transplanted with EC-induced MniPSC-MPP (1% GEMM of total CFUs), but not cells induced with cytokines alone (Figure 4C). To determine gene marking and confirm primate origin of hematopoietic colonies, CFC genomic DNA (gDNA) was assayed for NHP β-actin and LTR sequences (Figure 4D and Figure 5A; Supplemental Uncut Gel Image 2). The average gene marking in NHP β-actin+ CFUs and the number of gene-marked (LTR+) colonies were higher for mice transplanted with EC-induced versus cytokine-induced MniPSC-MPP.

To validate gene-modified MniPSC-MPP engraftment, we performed PCR analysis for detection of GFP (which is in the P140K transgene expression cassette) and monkey-specific Mn basigin (BSG) gDNA in engrafted mouse splenocytes. While Mn BSG was detected in splenic gDNA from all cohorts, GFP was detected only in EC-induced MniPSC-MPP transplant recipients (Figure 5B; Supplemental Uncut Gel Image 3). These findings confirm that engrafted cells originated from gene-modified EC-induced MniPSC-MPP that support effective in vivo selection, thereby increasing long-term engraftment.

EC-induced but not cytokine-induced PSC-MPP reconstitute myeloid and lymphoid compartments of secondary recipient mice. Serial transplantation of hematopoietic progenitor cells is the standard assay to confirm self renewal and multipotency prop-

Figure 6. Hypothetical model for vascular niche JAG1/DLL4-mediated induction of Notch activation of hematopoietic specification. Hemogenic cells ($CD34^+PECAM1^+VEC^+VEGFR^+$ $CD45^{lo/-}$) placed in a vascular niche that produces JAG1/DLL4 lead to Notch activation and upregulation of RUNX1 and GATA2, which, in combination with additional unknown factors (indicated by ??), support the endothelial-to-hematopoietic transition. Blockade of either JAG1 or DLL4 expression by vascular cells (shRNA to the membrane-bound Notch ligands) altered competing Notch-1, -2 ligand stoichiometry, reduced Notch activation in hemogenic precursors, lowered RUNX1 and GATA2 expression, and resulted in fewer $CD34^+CD45^+$ cells.

erties. We therefore transplanted first-degree BM into second-degree recipients (without intervening exposure to, coculture, or coinfusion with ECs). Multilineage engraftment and detection of lymphoid and erythroid cells in the blood 12 weeks after transplantation were higher in second-degree recipients of EC-induced MniPSC-MPP compared with recipients of cytokine-expanded cells (23% versus 11% $CD45^+$ cells) (Figure 5C). Importantly, the M/L ratio in second-degree recipients of EC-induced MniPSC-MPP was 1.2. In contrast, the M/L ratio for second-degree recipients of cytokine-induced MniPSC-MPP was 30 (myeloid skewed differentiation in vivo), which is closer to the typical M/L ratio observed for most human iPSC-MPP studies (i.e., M/L of 15) (4, 5). CFU assays indicated that BM from second-degree recipients' EC-induced hematopoietic cells had higher frequencies of erythroid and mixed hematopoietic colonies, and distribution of colony subtype resembled hematopoietic colony formation from second-degree recipients of Mn BM $CD34^+$ cells (Figure 5D). In contrast, BM from second-degree recipients of cytokine-induced cells did not give rise to mixed hematopoietic colonies and had a lower frequency of erythroid potential, which is consistent with the distribution of hematopoietic myeloid/erythroid subsets detected in the blood. These findings confirm long-term engraftment with authentic long-term hematopoietic progenitor cells generated from MniPSC hemogenic precursors by vascular niche induction. Furthermore, the engraftment level and in vivo contribution to hematopoiesis achieved with the EC-induced MPP strongly resemble the engraftment pattern achieved with human UCB-$CD34^+$ cell xeno-engraftment studies (16) and are significantly higher compared with the most effective hPSC-MPP engraftment studies to date (2, 4, 5).

Polyclonal reconstitution of secondary recipient mice transplanted with P140K-MniPSC LT-MPP. To confirm second-degree recipient gene-modified MniPSC-MPP repopulation, we conducted RIS analysis on gDNA from BM, spleen, and blood collected 28 weeks after infusion. Integration profiles indicated polyclonal repopulation without clonal dominance with the following: 25 clones identified across both cohorts; and 2 and 5 clones detected in undifferentiated parent MniPSC and second-degree recipients of "cytokine alone" and EC-expanded cells, respectively (Supplemental Tables 2 and 3). Thus, MniPSC $CD34^+$ cells instructed by human vascular niche contribute to long-term multilineage hematopoiesis without evidence of clonal dominance.

Discussion

Generation of LT-MPP from PSCs would greatly benefit patients with hematologic disease. Our studies mark a technical advance toward this goal, as we show long-term, high-level engraftment of "HSC-like cells" that we designated LT-MPP, based on Irv Weissman's gold standard that describes "HSCs" as "MPP" in human $CD34^+$ cell/mouse xenograft studies (39), in which more than 1 cell is transplanted into NSG mice.

In vivo selection tripled BM engraftment of hematopoietic progenitors that were induced with ECs in the presence of cytokines, while, in contrast, engraftment of cytokine alone–induced hematopoietic cells decreased over time and was skewed toward myeloid progeny in second-degree recipient mice. Importantly, EC-induced cells exhibited multipotency and self-renewal properties, as evidenced by multilineage reconstitution of both first-degree and second-degree recipients.

The critical role of the vascular niche for acquisition of self renewal and multipotent properties of hematopoietic progenitor cells that persist in vivo is supported by the evidence that cytokine-induced cells have significantly lower engraftment and restricted long-term myeloid potential ($P < 0.05$). Our study also reveals a direct role for the EC membrane–bound Notch ligands (JAG1 and DLL4) in definitive hematopoietic specification. However, the vascular niche may also play a role in engraftment of EC-induced MPP in the BM. From our unpublished observations, in which we found that coinfusion of vascular cells with cytokine-induced hematopoietic progenitors is not sufficient to produce LT-MPP, we hypothesize that cotransplantation of the vascular niche with the EC-induced MPP provides engraftment support such that the hematopoietic cells can successfully lodge in the BM, leading to higher basal repopulating ability. Successful lodgement in the BM and the initial support provided by niche cells allows for maturation of the cells to fully functional LT-MPP. Thus, transitioning EC-induced cells from a vascular ex vivo niche to a BM microenvironment supports maturation of LT-MPP.

In our proposed model, an ex vivo vascular niche produces JAG1 and DLL4, which activate Notch signaling in hemogenic precursors ($CD34^+PECAM1^+VEC^+VEGFR2^+CD45^{lo/-}$) to increase expression of RUNX1 and GATA2. This increased expression of RUNX1 and GATA2 in combination with other undefined factors supports the endothelial-to-hematopoietic transition. Blockade of either EC JAG1 or DLL4 expression (shRNA to these Notch ligands) reduced Notch activation in hemogenic precursors, lowered *RUNX1* and *GATA2* expression, and resulted in fewer $CD34^+CD45^+$ cells (Figure 6). In the historical context of published literature, which shows that direct modulation of either *RUNX1* or *GATA2* is not sufficient to generate LT-MPP, our work shows that direct contact between PSC-derived hemogenic precursors and a vascular niche is required for definitive hematopoiesis and production of LT-MPP. Our findings agree with results from other groups that indicate that Notch signaling is required for hematopoiesis (40). However, in those previously published studies, Notch activation by exposure to plastic-immobilized ligand

alone or in the context of a stromal cell culture is not sufficient for generation of definitive LT-MPP, given that PSC-derived hematopoietic cells generated under these conditions did not repopulate the BM long-term (23, 41).

Although vascular niche induction with Notch activation is required for definitive hematopoiesis, we recognize that there are likely additional unidentified acellular paracrine or autocrine factors produced by emergent HSCs and niche cells that are required for definitive hematopoiesis. The HSC-like cells generated in our ex vivo vascular niche functionally and phenotypically resemble more mature definitive multipotent progenitors ($CD34^+CD45^+CD41^-$) that emerge from hemogenic endothelium in the ventral wall of the dorsal aorta in the aorta-gonad-mesonephros (AGM) region of the developing embryo (6, 42). These cells are functionally (long-term engrafting, with lymphoid, myeloid, and erythroid potential) and phenotypically ($CD41^-$) distinct from the more primitive yolk sac or early emergent AGM embryonic hematopoietic progenitors ($CD41^+$) that are myeloerythroid restricted and transient, or immature, respectively (42, 43). While the vascular niche–induced hematopoietic progenitors differentiated from PSCs in our ex vivo systems strongly resemble definitive HSCs, we hypothesize that placing the $CD34^+$ hemogenic precursors in the BM milieu during hematopoietic specification is required for their maturation to definitive adult LT-MPP. We recognize, though, that the ex vivo vascular niche system likely requires further interrogation for successful and efficient large-scale production of authentic LT-MPP for transplantation and for translation to the clinic.

A more recent study in the zebrafish model indicated that the Notch-1 receptor is required for the endothelial to hematopoietic transition and HSC emergence from hemogenic endothelium (10). We previously showed that the mechanism of adult regenerative and homeostatic LT-MPP expansion in the mouse BM is through the endothelial JAG1/hematopoietic Notch-1 signaling axis, which balances self renewal and prevents adult HSC exhaustion after transplantation (14). Here, we show that endothelial Notch-1 ligands JAG1 and DLL4 are required for HSC emergence and support generation of LT-MPP from human and monkey PSCs during development. Although no direct connection between Notch signaling and *RUNX1* has been described previously, *RUNX1* has been shown to rescue hematopoiesis in the context of Notch-1 receptor deficiency (44), implying a link between the 2 pathways. Here, we show a direct relationship between loss of Notch-1 activation and loss of *RUNX1* expression, which directly links the 2 pathways.

Given that the endothelial Notch-1 ligands JAG1 and DLL4 are required for LT-MPP emergence from PSCs, one potential strategy to further improve PSC-MPP expansion in the future is through careful titration of endothelial Notch ligands JAG1 and DLL4 by genetic manipulation of ECs. Our engraftment levels are 5- to 20-fold higher compared with previous hPSC-MPP studies, and therefore our study represents an advance that will facilitate clinical translation of pluripotent blood stem cell therapeutics. Importantly, clinical applications of EC technology for human HSC expansion and transplantation in the clinic are forthcoming and the described P140K selection strategy has been safely and effectively applied in a clinical setting (38, 45); therefore, our strategy for LT-MPP generation should allow for a rapid translation to clinical studies following further appropriate preclinical scale-up and safety studies in the autologous primate model. Our work marks an advance in elucidating the mechanism of HSC emergence for developing an effective strategy for generation of LT-MPP for clinical application of human pluripotent blood stem cell therapeutics.

In vivo selection stabilized engraftment (up to 45%) at a level far above the therapeutic threshold (10%) for clinical benefit from gene therapy. EC Notch activation and increased *RUNX1* and *GATA2* expression are critical for generation of hematopoietic progenitors that can lodge and mature in the BM. Transplantation of hemogenic precursors that developed in coculture with a vascular niche to an in vivo BM niche supports their maturation from precursor to LT-MPP. The ability of LT-MPP to support in vivo selection further confirms their HSC-like status, as BCNU is an HSC-focused selection agent and does not appear to improve engraftment of hematopoietic cells specified ex vivo with cytokines alone.

Transcriptional profiling also identified differential expression of Wnt signaling pathway components in EC-educated MPP. Wnt signal strength has been shown to control the balance between self renewal and differentiation (46). We found that EC-educated MniPSC-MPP downregulated targets of the Wnt/β-catenin pathway relative to EC-naive MniPSC-MPP, which is not surprising given that ECs express Wnt pathway inhibitors *DKK1* (47), *DKK3* (15), *IGFPB2* (48), and *IGFBP3* (49). Wnt signaling has been shown to regulate the Notch pathway in normal (50–52) and malignant hematopoiesis (53, 54). The intersection between Wnt and Notch signaling and modulation of their equilibrium in the context of a vascular setting may reveal the precise balance required for endothelial to hematopoietic transition and definitive HSC emergence.

Endothelial JAG1 and DLL4/Notch-1 activation drive *RUNX1* and *GATA2* expression and hematopoietic specification of human and NHP PSCs, which highlights 2 important advances in clinical translation of pluripotent blood stem cell therapeutics: (a) JAG1 and DLL4 Notch-1 activation in the setting of vascular instruction directs the emergence of LT-MPP, and (b) P140K-mediated in vivo selection stabilizes engraftment of PSC-derived MPP, neither of which has, to our knowledge, been previously reported. Our work therefore represents an advance toward preclinical translation of PSC-based blood cell therapeutics in the NHP model and hPSCs, emphasizing a prominent role of the vascular niche in HSC development.

Methods

PSC lines. NHP MniPSC-7 and MniPSC-3 (17) (generated in our laboratory) were used in these studies and maintained as previously described (17, 55). The hESC line hes2 (NIH code ES02) was purchased from WiCell. MniPSC and hes2 cells were maintained on irradiated mouse embryonic fibroblasts (Chemicon) in DMEM:F12 medium, supplemented with 2 mM L-glutamine, 1% MEM nonessential amino acids, 20% KnockOut Serum Replacement, 100 μM 2-mercaptoethanol (Sigma-Aldrich), and 20 ng/ml bFGF (all reagents from Life Technologies unless noted). Cells were routinely monitored for PSC morphology and expression of pluripotency markers SSEA-4 and Oct4 (by flow cytometry) and tested negative for mycoplasma (Boca Scientific). For all assays, MniPSC and hes2 hESC were between passages 60 and 70.

NHP animal care. Healthy juvenile macaques (*M. nemestrina*), which are donors for BM $CD34^+$ cells used as positive controls in these studies, were housed at the University of Washington Regional Pri-

mate Research Center under conditions approved by the American Association for the Accreditation of Laboratory Animal Care.

Mouse animal care. Eight-week-old male NSG immunodeficient mice were housed at the FHCRC.

Macaque BM CD34⁺ cells. BM CD34⁺ cells were harvested and enriched from pigtail macaque BM as previously described (56).

Lentivirus vector production. Self-inactivating (SIN) lentivirus vectors and pRSC-EMPGW vector stock preparation have been described previously (57). The vector pRSC-EMPGW contains the human short elongation factor-1 α (EFS) promoter regulating the P140KMGMT chemotherapy resistance transgene (P140K).

Generation and use of E4ORF1-transduced ECs. Isolation, culture, and primary *E4ORF1* gene transfer into primary endothelium have been described previously (58). Primary ECs were isolated from human umbilical cords by members of the Jason Butler laboratory and transduced with E4ORF1-containing lentivirus vector per the referenced protocol listed above. For some experiments, E4ORF1 ECs were a gift from Angiocrine Bioscience (VeraVecs). ECs were passaged at ratios of 1:2 to 1:4 based on density, and passages 5 to 13 were used for PSC-MPP expansion studies. All cell lines were routinely tested for mycoplasma and were negative. In some experiments, ECs were also transduced with lentivirus vector expressing either shRNA to human JAG1 or shRNA to human DLL4.

Hematopoietic induction and differentiation. Hematopoietic mesoderm induction and differentiation of MniPSC lines were performed as described previously (17). On day 0, cells were treated with 10 μM Rock Inhibitor &-27632 (Stem Cell Technologies) in PSC media for 1 hour. Cells were then treated with 200 U/ml collagenase IV (Life Technologies), washed with DMEM:F12, and then aggregated in DMEM:F12 by scraping monolayers into cell clusters with a pipette. Cell clumps were resuspended in StemPRO media (Life Technologies) supplemented with StemPRO supplement, 2 mM L-glutamine, 1% penicillin-streptomycin (Life Technologies), 50 μg/ml ascorbic acid (Sigma-Aldrich), 150 μg/ml transferrin (Roche), and 4×10^{-4} M 1-thioglycerol (Sigma-Aldrich) with 10 ng/ml (hes2) or 20 ng/ml (MniPSC) of human BMP4 (R&D Systems). Aggregates were plated in 10-cm low cluster plates (Corning) and cultured at 37°C in hypoxia (5% O_2 in air) for 7 days. On day 1, EBs were settled in 15 ml conical tubes to remove dead single cells and then resuspended in supplemented StemPRO media containing BMP4, 2 μM 16, 16-dimethyl PGE2 (Cayman Biochemicals), and 10 ng/ml bFGF. On day 4, cells were replated in supplemented StemPRO containing 10 ng/ml VEGF, 2 μM PGE2, and 10 ng/ml bFGF. On day 8, EBs were dissociated into single cells with accutase (Life Technologies) and enriched for CD34⁺ cells using the EasySep Human PE Positive Selection Kit according to the manufacturer's instructions (Stem Cell Technologies). Cells were stained with 3 μg/ml anti-CD34 antibody conjugated with phycoerythrin (PE) (clone 563, BD Biosciences) and selected for PE⁺ cells per the manufacturer's protocol. Enriched cells were expanded for 7 days as described below. These differentiation studies were conducted on 2 MniPSC lines (3 and 7) and 1 hESC line (hes2) in 6 independent experiments per cell line.

PSC-derived MPP expansion. Sorted CD34⁺ cells were expanded with or without coculture on ECs in StemSpan SFEM media (Stem Cell Technologies) supplemented with 1% v/v penicillin-streptomycin (Life Technologies), 200 ng/ml stem cell factor (SCF) (Miltenyi Biotech), 100 ng/ml each of FLT-3 ligand (FL) (Peprotech) and thrombopoietin (TPO) (Peprotech), 50 ng/ml IL-11, 25 ng/ml IGF-1 and IGF-2, and 10 ng/ml b-FGF (Life Technologies). All growth factors are recombinant human and from R&D Systems unless otherwise noted. Hematopoietic/EC cocultures (EC and PSC-CD34⁺ cells) were cultured at 37°C in normoxia (20% O_2 in air) at a 3:1 ratio by cell density. After 7 days, adherent and suspension cells were harvested with accutase and processed for phenotypic or functional assays or for engraftment studies.

Ex vivo selection of MniPSC-derived hematopoietic cells. O^6BG (Sigma-Aldrich) was reconstituted in DMSOv (Sigma-Aldrich) solution to a concentration of 50 mM. BCNU (Sigma-Aldrich) was reconstituted to 155 mM concentration in ethanol. Day-8 CD34⁺ MPP were subjected to ex vivo drug selection with indicated concentrations of O^6BG or equivalent volumes of DMSO as vehicle controls and incubated at 37°C (5% CO_2, 20% O_2) for 1 hour, followed by addition of indicated concentrations of BCNU or equivalent volumes of ethanol as vehicle controls. Chemotherapy- and vehicle-treated cells were then plated in standard CFC assays (see below).

Colony formation in methylcellulose. Short-term CFC assays were performed as described previously (17). Briefly, cells were plated in Methocult H4230 (Stem Cell Technologies) supplemented with the following cytokines: 100 ng/ml each of SCF, TPO, GM-CSF, G-CSF, IL-3, IL-6, and 4 U/ml erythropoietin (EPO). After 12 days, plates were scored for hematopoietic colony phenotypes (CFU-E, CFU-M CFU-GM, CFU-GEMM) under a light microscope. Individual colonies from each experiment were randomly picked for Wright-Giemsa staining of cytospin samples and, in some studies, for analysis of proviral integration by PCR assay (56).

RNA isolation and real-time qRT-PCR. RNA isolation and real-time qRT-PCR have been previously described (17). Macaque-specific (human cross-reactive) primers designed based on the annotated rhesus macaque genome where possible are either listed in Supplemental Table 1 or have been previously described (17).

Flow cytometry analysis. Flow cytometry analysis was performed using standard procedures (17). All antibodies are from BD Biosciences unless otherwise indicated. Macaque BM and peripheral blood white blood cells and MniPSC–derived cells were stained with the following antibodies in different combinations: mouse anti-human (NHP cross-reactive) CD34-PE (clone 563, catalog no. 550761), CD34-APC (clone 563, catalog no. 561209), CD45-PerCP (clone TU116, catalog no. 557513) and NHP-specific (not cross-reactive with human) CD45-BV786 (clone D058-1283, catalog no. 563861), CD45-APC (clone D058-1283, catalog no. 561290), anti-human CD45-eFLUOR450 (eBioscience clone 2D1, catalog no. 48-9459), and NHP-specific (not cross-reactive with human) CD38-APC (NHP Reagent Resource). MPP and ECs were also stained with KDR-PE (R&D Systems, catalog no. FAB357P), CD31-V450 (clone WM59, catalog no. 561653), CD31-PE (clone WM59, catalog no. 555446) and CD31-APC (clone WM59, eBioscience catalog no. 17-0319), CD144-APC (VE-cadherin; eBioscience clone 16B1 catalog no. 17-1449) and CD144–Alexa Fluor 700 (eBioscience clone 16B1, catalog no. 56-1449) and Tra-1-85-APC (R&D Systems catalog no. FAB3195A). In coculture systems, ECs were distinguished from MniPSC-MPP by forward and side scatter, expression of the pan-human antigen CD147 (which is encoded by the human *BSG* gene), and identified by immunostaining with the Tra-1-85 antibody. For in vivo studies, cells were costained with a human/NHP-specific antibody (anti-human CD45 PerCP and anti-primate CD45-BV786 or anti-human CD45 APC Cy7), a mouse CD45-specific antibody (anti-mouse CD45 FITC, eBiosciences clone 30-F11, catalog no.

11-0451 or anti-mouse CD45 V450, eBioscience clone 30F11, catalog no. 48-0451), CD14-PeCy7 (clone M5E2, catalog no. 560919), CD3-APC (clone SP34-2, catalog no. 557597), CD3–Alexa Fluor 488 (clone SP34-2, catalog no. 557705), CD20 Brilliant Violet 605 (Biolegend, clone 2H7, catalog no. 302333), and CD235ab Pacific Blue (Biolegend clone HIR2, catalog no. 306611). For in vivo studies, human-specific antibodies reported to be cross-reactive with monkey blood cells were selected; then a gating strategy was established and applied to all in vivo analyses. Mouse peripheral samples were also stained with anti-mouse CD45-FITC or mouse CD45-eFlour-450 (eBioscience). To detect erythroid cells, cells were costained with anti-human CD235ab and anti-HbF (Life Technologies, clone HbF-1, catalog no. MHFH05) antibodies (adult macaque blood, unlike adult human blood, contains HbF) (59).

Western blot analysis. Western blot analysis of MGMT protein expression has been described elsewhere (38). Primary antibody staining was performed with anti-human MGMT (Kamiya Biomedical) at a dilution of 1:500 or β-actin (N-21) (Santa Cruz Biotechnology Inc.) at a dilution of 1:200 for 1 hour at room temperature (RT). The secondary antibodies used were goat anti-mouse (BD Biosciences) or goat anti-rabbit (R&D Systems) immunoglobulin G1 conjugated to horseradish peroxidase, respectively, at a dilution of 1:2,000 for 1 hour at RT. The immunoblotted complex was visualized using the Kodak X-OMAT 2000 Processor.

Real-time qPCR (TaqMan). Gene marking in transduced PSCs and their hematopoietic progeny was analyzed by TaqMan 5′ nuclease real-time qPCR assay as described previously (37). Sample DNA was analyzed in duplicate with a lentivirus-specific primer/probe combination (forward, 5′-TGAAAGCGAAAGGGAAACCA; reverse, 5′-CCGTGCGCGCTTCAG; probe, 5′-AGCTCTCTCGACGCAGGACTCGGC [IDT]) and in a separate reaction with a β-globin–specific primer/probe combination (forward, 5′-CCTATCAGAAAGTGGTGGCTGG; reverse, 5′-TTGGACAGCAAGAAAGTGAGCTT; probe, 5′-TGGCTAATGCCCTGGCCCACAAGTA [DT]) to adjust for equal loading volume of gDNA per reaction.

Transplantation studies in NSG mice. Mice received a sublethal dose of irradiation from a Cesium source (275 cGy) 1 day before transplantation. For the PGE2 pulse, day-15 cocultures were manually processed to single-cell suspension, washed with DPBS, and resuspended in StemSpan containing 10 μM PGE2. Cells were placed on ice (at room temperature) for 2 hours and vortexed every 30 minutes. After PGE2 treatment, cells were washed twice with DPBS, passed through a 70-micron filter, loaded into a 0.5 cc insulin syringe, and injected directly into the right femurs of anesthetized mice. Experiment 1 and 2 cell doses were as follows: MniPSC-MMP EC coculture, 0.3 million MniPSC-MPP and 0.9 million ECs (experiment 1: $n = 3$ mice/group; experiment 2: $n = 12$ mice/group); 0.3 million cytokine alone–induced MPP ($n = 8$ mice/group); Mn BM $CD34^+$ MPP, 2 million cells ($n = 8$ mice). Experiment 3 cell doses included the following: cytokine-expanded P140K-MniPSC-MPP, 0.35 million ($n = 7$ mice); EC-expanded P140K-MniPSC-MPP, 0.35 million MPP, and 1 million ECs ($n = 12$ mice).

For Experiment 1 (Figure 1) (engraftment of MPP induced with cytokines ± Notch ligand–replete or –deficient ECs), engraftment was evaluated 12 weeks after injection. To study long-term engraftment in experiment 2 (Figure 2), mice were monitored weekly for 16 to 24 weeks by flow cytometry for detection of NHP $CD45^+$ cells and myeloid, lymphoid, and erythroid progeny in the $CD45^+$ gate.

For experiment 3, which studies the long-term effect of in vivo selection on engraftment of cytokine-induced and EC-induced MPP, both primary and secondary BM transplants were conducted. For secondary BM transplantation assays, whole BM was collected from 16-week engrafted primary recipients and directly injected into the BM of sublethally irradiated (275 cGy) secondary recipients (BM from 1 primary donor into 1 secondary recipient) ($n = 3$ secondary recipients per group). Cells were infused without any intervening additional culture period and without any additional ECs. Secondary recipients were analyzed 12 weeks after transplantation.

Chemotherapy preparation and administration to NSG mice. O^6BG (50 mg bottle, Sigma-Aldrich) was resuspended in 3.33 ml PEG-400 (Sigma-Aldrich) and sonicated in warm water for 40 minutes. O^6BG was then diluted with DBPS to a final concentration of 5 mg/ml in 10 ml final volume. BCNU (Carmustine, 25 mg vial, Sigma-Aldrich) was reconstituted in 0.75 ml 100% ethanol at a final concentration of 33.3 mg/ml. Mice received 2 i.p. injections of O^6BG at a dose of 5 mg/kg per injection, with the 2 injections fractionated 30 minutes apart (total dose 10 mg/kg). One hour after the first O^6BG injection, mice received an i.p. injection of BCNU at a dose of 1 mg/kg or 2 mg/kg. To assess myelosuppression, mice were monitored by complete blood count (CBC) analysis immediately before and up to 2 weeks after chemotherapy administration.

Analysis of PSC-derived cell engraftment in hematopoietic organs. Following euthanasia of mice, femurs, tibia and iliac crests, spleen, liver, and blood were harvested for preparation of single-cell suspensions as described elsewhere (2). Based on yield, cells from individual mice and organs were divided for gDNA extraction, RNA extraction, flow cytometry analysis, and CFC assays. $CD3^+$ and $CD14^+$ cells were isolated from spleen and BM, respectively, of transplanted mice. Spleen-derived primate lymphocytes were cultured in T cell–supportive medium (17) and activated with CD3/CD28 magnetic beads for 1 to 2 weeks. BM-derived primate monocytes were differentiated into macrophages as described (60). Cytokine production by the organ-derived cells was analyzed using the NHP Th1/Th2 cytokine kit (cytokine bead array, BD Biosciences) according to the manufacturer's instructions.

PCR amplification and analysis of gDNA from hematopoietic CFCs. Hematopoietic colonies generated from mouse organs (24 colonies per organ [BM, spleen, liver] per mouse) were isolated and transferred to tubes containing 90 μl of water supplemented with 1.7 U of proteinase K from *Tritirachium album* (Sigma-Aldrich). GDNA was isolated from individual colonies and then subjected to PCR analysis to determine percentage of colonies containing the lentiviral provirus and NHP gDNA. To validate NHP origin of hematopoietic colonies, multiple PCR reactions were performed on gDNA extracted from each colony with NHP- and human-specific PCR primers for detection of β-actin, β-globin (NHP, human), and BSG (pan-human specific gDNA encoding the human CD147 antigen). Primer sequences are listed in Supplemental Table 1.

RIS analysis. RIS amplification, detection, and processing were carried out as previously described, with the exception of random shearing, which was accomplished by adaptive focused acoustics technology (38). Briefly, 3 μg of DNA from each sample was sheared using the M220 focused ultrasonicator (Covaris). Fragmented DNA was isolated and polished, and modified linkers were ligated following the manufacturer's protocol (454/Roche-GS 20 DNA library preparation kit). About 100 to 200 ng of double-stranded DNA was

then amplified in a standard exponential PCR (primer pair 1, LTR-specific L2-PST-1-5′-biotin-AGCTTGCCTTGAGTGCTTCA-3′ and linker-specific LC1 1-5′-GACCCGGGAGATCTGAATTC-3′; primer pair 2, 2A-[Barcode]- LTR-specific L2: 5′-CCATCTCATCCCTGCGTGTCTCCGACTCAG-[Barcode]-AGTAGTGTGTGCCCGTCTGT-3′ and linker-specific LC2-trP1- 5′-CCTCTCTATGGGCAGTCGGTGATGATCTGAATTCAGTGGCACAG-3′). LTR-specific primer L2-PST-1 was biotin tagged to capture/wash specific products from the first PCR, and DNA was diluted 1:100 in H_2O before a second, nested PCR with barcoded, LTR-specific, and modified linker-specific primers was fused to sequences for compatibility to massively paralleled semiconductor sequencing (IonTorrent; Invitrogen/Life Technologies). PCR products were visualized on a 2% agarose gel, and DNA fragments ranging from approximately 300 to 800 bp were gel purified and sequenced by the semiconductor sequencing service available from Edge Biosciences following standard procedures. Processing and genomic mapping of retrovirus integration sites were carried out as previously described (38) with the following exceptions: valid integration sites were scored after locating retrovirus LTR-intervening NHP gDNA and linker cassette sequence. The resulting junction sequences were aligned to the October 2010 (BGI CR_1.0/rheMac3) assembly of the rhesus genome with a stand-alone version of BLAT that generates a BLAST alignment score. To assign the closest transcription start site (TSS) proximal to the site of virus integration, the flanking NHP genomic sequence identified was converted to the corresponding sequence in the human genome by aligning to the February 2009 (GRCh37/hg19) genome assembly, which was then interrogated for the nearest RefSeq gene TSS.

RNA-Seq library construction, sequencing, and analysis. RNA preparation, library construction, sequencing, and analysis were performed as previously described (61). All original RNA-Seq data were deposited in the NCBI's Gene Expression Omnibus (GEO GSE64644).

Statistics. Means and SD were calculated and Student's *t* tests performed where indicated using Microsoft Excel software version 14.14.6. $P < 0.05$ was considered significant.

Study approval. The mouse animal procedures conformed to protocols approved by the FHCRC Institutional Animal Care and Use Committee. The NHP studies (collection of peripheral blood cells and BM $CD34^+$ cells) were conducted under protocols approved by the Institutional Review Board and Animal Care and Use Committees of the University of Washington.

Acknowledgments

We thank Grace Choi for help in preparing this manuscript and Brian Beard, Emily Menard, Christina Ironside, and Krystin Norman for technical assistance at FHCRC. We also thank Cyd Norgiat, Melissa Comstock, and LaKeisha Perkins for assistance with the animal work. We thank the Comparative Medicine Department, Flow Cytometry Shared Resource Facility at FHCRC. We thank Grant Trobridge at Washington State University for work on RIS data processing. We thank Sunita D'Souza and the Human Embryonic Stem Cell/Induced Pluripotent Stem Cell Shared Resource Facility for providing quality controlled reagents for PSC cell culture and hematopoietic differentiation. This work was supported in part by NIH grants HL098489, HL085693, HL084345, and HL115128. H.P. Kiem is a Markey Molecular Medicine Investigator and received support as the inaugural recipient of the José Carreras/E.D. Thomas Endowed Chair for Cancer Research. S. Rafii is a Howard Hughes Medical Institute Investigator.

Address correspondence to: Hans-Peter Kiem, Fred Hutchinson Cancer Research Center, D1-100, P.O. Box 19024, Seattle, Washington 98109-1024, USA. Phone: 206.667.4425; E-mail: hkiem@fhcrc.org.

1. Tian X, Woll PS, Morris JK, Linehan JL, Kaufman DS. Hematopoietic engraftment of human embryonic stem cell-derived cells is regulated by recipient innate immunity. *Stem Cells*. 2006;24(5):1370–1380.
2. Ledran MH, et al. Efficient hematopoietic differentiation of human embryonic stem cells on stromal cells derived from hematopoietic niches. *Cell Stem Cell*. 2008;3(1):85–98.
3. Risueno RM, et al. Inability of human induced pluripotent stem cell-hematopoietic derivatives to downregulate microRNAs in vivo reveals a block in xenograft hematopoietic regeneration. *Stem Cells*. 2012;30(2):131–139.
4. Doulatov S, et al. Induction of multipotential hematopoietic progenitors from human pluripotent stem cells via respecification of lineage-restricted precursors. *Cell Stem Cell*. 2013;13(4):459–470.
5. Amabile G, et al. In vivo generation of transplantable human hematopoietic cells from induced pluripotent stem cells. *Blood*. 2013;121(8):1255–1264.
6. Kissa K, Herbomel P. Blood stem cells emerge from aortic endothelium by a novel type of cell transition. *Nature*. 2010;464(7285):112–115.
7. Wei Y, Ma D, Gao Y, Zhang C, Wang L, Liu F. Ncor2 is required for hematopoietic stem cell emergence by inhibiting Fos signaling in zebrafish. *Blood*. 2014;124(10):1578–1585.
8. Zhen F, Lan Y, Yan B, Zhang W, Wen Z. Hemogenic endothelium specification and hematopoietic stem cell maintenance employ distinct Scl isoforms. *Development*. 2013;140(19):3977–3985.
9. Liakhovitskaia A, et al. Runx1 is required for progression of $CD41^+$ embryonic precursors into HSCs but not prior to this. *Development*. 2014;141(17):3319–3323.
10. Kim AD, et al. Discrete Notch signaling requirements in the specification of hematopoietic stem cells. *EMBO J*. 2014;33(20):2363–2373.
11. Nolan DJ, et al. Molecular signatures of tissue-specific microvascular endothelial cell heterogeneity in organ maintenance and regeneration. *Dev Cell*. 2013;26(2):204–219.
12. Butler JM, et al. Endothelial cells are essential for the self-renewal and repopulation of Notch-dependent hematopoietic stem cells. *Cell Stem Cell*. 2010;6(3):251–264.
13. Ding L, Saunders TL, Enikolopov G, Morrison SJ. Endothelial and perivascular cells maintain haematopoietic stem cells. *Nature*. 2012;481(7382):457–462.
14. Poulos MG, et al. Endothelial jagged-1 is necessary for homeostatic and regenerative hematopoiesis. *Cell Rep*. 2013;4(5):1022–1034.
15. Kobayashi H, et al. Angiocrine factors from Akt-activated endothelial cells balance self-renewal and differentiation of haematopoietic stem cells. *Nat Cell Biol*. 2010;12(11):1046–1056.
16. Butler JM, Gars EJ, James DJ, Nolan DJ, Scandura JM, Rafii S. Development of a vascular niche platform for expansion of repopulating human cord blood stem and progenitor cells. *Blood*. 2012;120(6):1344–1347.
17. Gori JL, et al. Efficient generation, purification, and expansion of $CD34^+$ hematopoietic progenitor cells from nonhuman primate-induced pluripotent stem cells. *Blood*. 2012;120(13):e35–e44.
18. Zhong B, et al. Safeguarding nonhuman primate iPS cells with suicide genes. *Mol Ther*. 2011;19(9):1667–1675.
19. Zhong B, et al. Efficient generation of nonhuman primate induced pluripotent stem cells. *Stem Cells Dev*. 2011;20(5):795–807.
20. Reubinoff BE, Pera MF, Fong CY, Trounson A, Bongso A. Embryonic stem cell lines from human blastocysts: somatic differentiation in vitro. *Nat Biotechnol*. 2000;18(4):399–404.
21. Kennedy M, D'Souza SL, Lynch-Kattman M, Schwantz S, Keller G. Development of the hemangioblast defines the onset of hematopoiesis in human ES cell differentiation cultures. *Blood*. 2007;109(7):2679–2687.
22. Wang L, et al. Endothelial and hematopoietic cell

fate of human embryonic stem cells originates from primitive endothelium with hemangioblastic properties. *Immunity*. 2004;21(1):31–41.
23. Lee JB, et al. Notch-HES1 signaling axis controls hemato-endothelial fate decisions of human embryonic and induced pluripotent stem cells. *Blood*. 2013;122(7):1162–1173.
24. Wang L, et al. Generation of hematopoietic repopulating cells from human embryonic stem cells independent of ectopic HOXB4 expression. *J Exp Med*. 2005;201(10):1603–1614.
25. Sturgeon CM, Ditadi A, Awong G, Kennedy M, Keller G. Wnt signaling controls the specification of definitive and primitive hematopoiesis from human pluripotent stem cells. *Nat Biotechnol*. 2014;32(6):554–561.
26. Gori JL, et al. In vivo selection of human embryonic stem cell-derived cells expressing methotrexate-resistant dihydrofolate reductase. *Gene Ther*. 2010;17(2):238–249.
27. Benedito R, et al. The notch ligands Dll4 and Jagged1 have opposing effects on angiogenesis. *Cell*. 2009;137(6):1124–1135.
28. Chen MJ, Yokomizo T, Zeigler BM, Dzierzak E, Speck NA. Runx1 is required for the endothelial to haematopoietic cell transition but not thereafter. *Nature*. 2009;457(7231):887–891.
29. Marcelo KL, et al. Hemogenic endothelial cell specification requires c-Kit, Notch signaling, and p27-mediated cell-cycle control. *Dev Cell*. 2013;27(5):504–515.
30. de Pater E, et al. Gata2 is required for HSC generation and survival. *J Exp Med*. 2013;210(13):2843–2850.
31. Cutler C, et al. Prostaglandin-modulated umbilical cord blood hematopoietic stem cell transplantation. *Blood*. 2013;122(17):3074–3081.
32. Speth JM, Hoggatt J, Singh P, Pelus LM. Pharmacologic increase in HIF1alpha enhances hematopoietic stem and progenitor homing and engraftment. *Blood*. 2014;123(2):203–207.
33. Fares I, et al. Pyrimidoindole derivatives are agonists of human hematopoietic stem cell self-renewal. *Science*. 2014;345(6203):1509–1512.
34. Rongvaux A, et al. Human hemato-lymphoid system mice: current use and future potential for medicine. *Annu Rev Immunol*. 2013;31:635–674.
35. Broxmeyer HE, et al. Growth characteristics and expansion of human umbilical cord blood and estimation of its potential for transplantation in adults. *Proc Natl Acad Sci U S A*. 1992;89(9):4109–4113.
36. Trobridge GD, et al. Protection of stem cell-derived lymphocytes in a primate AIDS gene therapy model after in vivo selection. *PLoS One*. 2009;4(11):e7693.
37. Beard BC, Trobridge GD, Ironside C, McCune JS, Adair JE, Kiem HP. Efficient and stable MGMT-mediated selection of long-term repopulating stem cells in nonhuman primates. *J Clin Invest*. 2010;120(7):2345–2354.
38. Adair JE, et al. Extended survival of glioblastoma patients after chemoprotective HSC gene therapy. *Sci Transl Med*. 2012;4(133):133ra57.
39. Majeti R, Park CY, Weissman IL. Identification of a hierarchy of multipotent hematopoietic progenitors in human cord blood. *Cell Stem Cell*. 2007;1(6):635–645.
40. Kumano K, et al. Notch1 but not Notch2 is essential for generating hematopoietic stem cells from endothelial cells. *Immunity*. 2003;18(5):699–711.
41. Shojaei F, et al. Hierarchical and ontogenic positions serve to define the molecular basis of human hematopoietic stem cell behavior. *Dev Cell*. 2005;8(5):651–663.
42. McKinney-Freeman SL, et al. Surface antigen phenotypes of hematopoietic stem cells from embryos and murine embryonic stem cells. *Blood*. 2009;114(2):268–278.
43. Palis J, Robertson S, Kennedy M, Wall C, Keller G. Development of erythroid and myeloid progenitors in the yolk sac and embryo proper of the mouse. *Development*. 1999;126(22):5073–5084.
44. Nakagawa M, et al. AML1/Runx1 rescues Notch1-null mutation-induced deficiency of para-aortic splanchnopleural hematopoiesis. *Blood*. 2006;108(10):3329–3334.
45. Adair JE, et al. Gene therapy enhances chemotherapy tolerance and efficacy in glioblastoma patients. *J Clin Invest*. 2014;124(9):4082–4092.
46. Luis TC, Ichii M, Brugman MH, Kincade P, Staal FJ. Wnt signaling strength regulates normal hematopoiesis and its deregulation is involved in leukemia development. *Leukemia*. 2012;26(3):414–421.
47. van der Horst G, van der Werf SM, Farih-Sips H, van Bezooijen RL, Lowik CW, Karperien M. Downregulation of Wnt signaling by increased expression of Dickkopf-1 and -2 is a prerequisite for late-stage osteoblast differentiation of KS483 cells. *J Bone Min Res*. 2005;20(10):1867–1877.
48. Huynh H, et al. IGF binding protein 2 supports the survival and cycling of hematopoietic stem cells. *Blood*. 2011;118(12):3236–3243.
49. Oikonomopoulos A, et al. Wnt signaling exerts an antiproliferative effect on adult cardiac progenitor cells through IGFBP3. *Circ Res*. 2011;109(12):1363–1374.
50. Clements WK, Kim AD, Ong KG, Moore JC, Lawson ND, Traver D. A somitic Wnt16/Notch pathway specifies haematopoietic stem cells. *Nature*. 2011;474(7350):220–224.
51. Saint Just Ribeiro M, Hansson ML, Lindberg MJ, Popko-Scibor AE, Wallberg AE. GSK-3beta is a negative regulator of the transcriptional coactivator MAML1. *Nucleic Acids Res*. 2009;37(20):6691–6700.
52. Cheng X, Huber TL, Chen VC, Gadue P, Keller GM. Numb mediates the interaction between Wnt and Notch to modulate primitive erythropoietic specification from the hemangioblast. *Development*. 2008;135(20):3447–3458.
53. Rodilla V, et al. Jagged1 is the pathological link between Wnt and Notch pathways in colorectal cancer. *Proc Natl Acad Sci U S A*. 2009;106(15):6315–6320.
54. Chen X, Stoeck A, Lee SJ, Shih LM, Wang MM, Wang TL. Jagged1 expression regulated by Notch3 and Wnt/β-catenin signaling pathways in ovarian cancer. *Oncotarget*. 2010;1(3):210–218.
55. Seki T, Yuasa S, Fukuda K. Generation of induced pluripotent stem cells from a small amount of human peripheral blood using a combination of activated T cells and Sendai virus. *Nat Protoc*. 2012;7(4):718–728.
56. Trobridge GD, et al. Efficient transduction of pigtailed macaque hemtopoietic repopulating cells with HIV-based lentiviral vectors. *Blood*. 2008;111(12):5537–5543.
57. Horn PA, et al. Efficient lentiviral gene transfer to canine repopulating cells using an overnight transduction protocol. *Blood*. 2004;103(10):3710–3716.
58. Seandel M, et al. Generation of a functional and durable vascular niche by the adenoviral E4ORF1 gene. *Proc Natl Acad Sci U S A*. 2008;105(49):19288–19293.
59. Scott R, Anyaibe S, Yancey A, Headings V. Fetal hemoglobin distributions among adult baboon and macaque species. *Primates*. 1986;27(2):259–268.
60. Rozner AE, Dambaeva SV, Drenzek JG, Durning M, Golos TG. Generation of macrophages from peripheral blood monocytes in the rhesus monkey. *J Immunol Methods*. 2009;351(1–2):36–40.
61. Ginsberg M, et al. Efficient direct reprogramming of mature amniotic cells into endothelial cells by ETS factors and TGF-β suppression. *Cell*. 2012;151(3):559–575.